JOURNAL OF CHEMICAL ENGINEERING AND INDUSTRIAL BIOTECHNOLOGY
E-ISSN: 0126-8139
VOLUME 9, ISSUE 2, SEPTEMBER 2023, 48 – 57
DOI: https://doi.org/10.15282/jceib.v9i2.9495

UNIVERSITI MALAYSIA PAHANG AL-SULTAN ABDULLAH

RESEARCH ARTICLE

Molecular Dynamics Simulation Study of the Diffusion of Carbon Dioxide in Heptane: Application in Natural Gas Cleaning

A.S. Ahmed*, M.M. Ahmed, A.A. Bello

Department of Chemical Engineering, University of Maiduguri, PMB 1069, Borno State, Nigeria

ABSTRACT - Using solvents to remove carbon dioxide is an effective way to purify natural gas. Diffusion of solute in solvent is key to natural gas purification. In this study, molecular dynamics (MD) simulations of the diffusion of carbon dioxide in heptane at different temperatures and pressures were performed to simulate the conditions of industrial purification process. The diffusion coefficients were measured in two different configurations: pure solvent and binary solute-solvent systems. The diffusion coefficients of the binary system were observed to be in the order of 10-9 m2/s. An increased temperature was observed to increase the diffusion coefficient of the carbon dioxide in heptane while an increase in pressure reduced the value of the diffusion coefficient. The diffusion coefficient was also observed to follow an Arrhenius-type relationship with respect to temperature. The activation energy of the system increased from 9.228 kJ/mol to 11.139 kJ/mol with pressure increase. A linear relationship was detected between the diffusion coefficient and the viscosity of the system and an increased viscosity of the system results in a decreased diffusion coefficient. The results of the research showed that carbon dioxide behavior in heptane offers the theoretical backing for the development of a new natural gas desulphurization solvent.

ARTICLE HISTORY
Received : 25th Jul. 2023
Revised : 11th Sep. 2023
Accepted : 18th Sep. 2023
Published : 30th Dec. 2023

KEYWORDS
Molecular Dynamics
Ensemble
Diffusion Coefficient
Force Field
Arrhenius Equation
Activation Energy

1.0 INTRODUCTION

The world is now shifting towards fuels with low carbon content like natural gas for the generation of energy to meet global demand. Currently, about 80.7% of the global energy demand is being met by oil, natural gas and coal [1]. There is a significant expectance in the increase of natural gas consumption in the world with projections of about 6 trillion cubic metres by 2030 [2]. Estimates have shown that the change to fuels with low carbon content will reduce CO2 emissions by up to 15% by the year 2050 [3]. Natural gas is projected to be the most demanded energy component in the not too distance future. The annual usage of natural gas has been reported to be increasing by an average of 2.8% annually since 2001 compared to oil and coal having 1.8% and 1.5% respectively [4].

Methane is the major component of natural gas, amounting to about 95% of its composition and other components such as propane, butane, carbon dioxide, sulfur, etc., accounting for the rest. Due to methane being the major constituent, its properties are used to compare natural gas to other fuels [5]. CO2 has been considered as the key player when it comes to global warming. Thus, fuels are mostly categorized as non-environmentally friendly due to their contribution of CO2 to the atmosphere. Out of the available fossil fuels, natural gas has the least contribution of CO2 to the atmosphere, making it the cleanest burning fossil fuel [6]. Due to the cleanliness of natural gas, concerns have risen for the usage of fuels such as compressed or liquefied natural gas for vehicles [7]. It is known that the energy content of gaseous fuels is less than liquid fuels, however the traveling distance of urban vehicles is short and there is the availability for the option of refueling [8]. With this regard, the exhaust from natural gas-powered vehicles will have less emission compared to an equivalent gasoline vehicle. According to the report by Demirbas [9], natural gas vehicles have 70% lower emission of carbon dioxide compared to petroleum vehicles. To further understand the mass transfer process in the absorption process, the diffusion coefficient must be accurately determined.

The diffusion coefficient is one of the physical properties that is very important in transport phenomena due to its application in chemical processes such as extraction and in the design of chemical processes. With regards to that, the determination of the diffusion coefficient, especially of compounds in organics such as alkanes, is vital in the design of chemical processes and study of mass transfer in such systems [10]. Diffusion coefficient among other properties such as heat capacity and density are critical in the design and study of unit operation equipments such as reactors and absorbers [11]. These values are in most cases experimentally determined. However, experiments are mostly expensive to carry out and time-consuming. These challenges have been reported in determining diffusion coefficient, especially at low concentrations, which subsequently led to the use of theoretical or precise computational methods when carrying out such analysis [12].

In this work, the diffusion coefficient was calculated using the Molecular Dynamics (MD) method. Empirical correlations were used to determine the diffusion coefficients at the selected conditions for comparison. The Arrhenius

*CORRESPONDING AUTHOR | A.S. Ahmed | ✉ ahmedsadiq52@yahoo.com

relation was used to determine the relationship between the diffusion coefficient and temperature. Other properties like viscosity and density were also investigated to determine their relationship with the diffusion coefficient. It is hoped that the results and analysis will aid in the investigation of CO_2 removal to improve systems comprising of such.

2.0 METHODS AND MATERIAL

2.1 Molecular Dynamics Setup

The simulations were conducted using the Groningen Machine for Chemical Simulation (GROMACS) simulator. For the CO_2 molecule the modified SPC force field used by Kamath, et al. [13] was adopted while for the heptane molecule the OPLS-AA force field was used and these force fields were used due to their accuracy and efficiency. The periodic boundary condition was implemented for the mixture system, this helps to prevent the surface effect as well as maintain the number of specified molecules within the simulation box. The intermolecular interaction is represented by the Lenard-Jones and the Coulombic interaction [14] given by Eqn.(1) and Eqn. (2) respectively.

$$V_{LJ} = \sum_{ij} 4\varepsilon_{ij}\left[\left(\frac{\delta_{ij}}{r_{ij}}\right)^{12} - \left(\frac{\delta_{ij}}{r_{ij}}\right)^{6}\right] \tag{1}$$

For an atomic pair of i and j, ε is the potential well depth, δ signifies the distance where there is no potential between the atomic pairs and r is the length between the atomic centres of the two atoms [15].

$$v_c = \sum_{ij} \frac{1}{4\pi\varepsilon_0}.\frac{q_i q_j}{r_{ij}} \tag{2}$$

The q_i and q_j are the point charges of the atomic pair i and j respectively, r_{ij} is the distance between the centre of the particles and ε_0 is the permittivity of free space. The electrostatic potential has both short and long range interactions, unlike the Lennard Jones potential these long range interactions cannot be discarded as they are very effective in many cases [16].

The cut off used for the Lennard-Jones potential and the Coulombic interactions are 12Å and 8.5Å respectively. The mixing rule used for the pair coefficients is the Lorentz-Bethelot mixing rule [17] given by Eqn. (3) and (4).

$$\sigma_{12} = \frac{\sigma_1+\sigma_2}{2} \tag{3}$$

$$\varepsilon_{12} = \sqrt{\varepsilon_1\varepsilon_2} \tag{4}$$

where σ *and* ε are given in Å and eV respectively.

The whole simulation was carried out using the GROMACS simulator. The simulation was initiated by minimizing the energy of the system using the steepest descent algorithm. The system was then subjected to an NVT equilibration followed by an NPT equilibration for 1ns each to control the temperature and pressure of the system respectively. The system was then subjected to a final production run in the NVT ensemble for 4ns to generate enough data to help compute the property of interest. The system configuration after both equilibrations was optimal under the selected temperature and pressure as the temperature and density of the system were observed to stabilize within the specified values. The v-rescale thermostat and Parinello-Rahman barostat were respectively used to control the system temperature and pressure.

2.1 Model Used

The mean square displacement (MSD) method which was developed using the Einstein relation was used to calculate the diffusion coefficient. The equation relates the MSD of a given molecule to the time taken for diffusion as shown in Eqn. (5).

$$D = \lim_{t\to\infty} \frac{\langle[r_i(0)-r_i(t)]^2\rangle}{6t} \tag{5}$$

where r_i is the position vector of the CO_2 molecule and t is the time. The coefficient was calculated on an ensemble average over all the CO_2 molecules and times.

Standard error (Eqn. (6)) was used to determine the error range as multiple runs are conducted for improved statistics.

$$\sigma_x = \frac{\sigma}{\sqrt{n}} \tag{6}$$

where σ is the standard deviation and n is the sample size. The standard error is used to compute the error for the average simulation results used with respect to the individual sample population.

3.0 RESULTS AND DISCUSSION

3.1 Analysis of Pure Solvent

Prior to carrying out the simulation of the system mixture, the selected parameters such as the force field, the computational method, topology of the simulation, etc. need to be validated. To achieve this, the pure solvent (heptane) was simulated at a pressure of 1bar and temperatures of 288K – 368K and its thermodynamic property (in this case the density and the diffusion coefficient) were observed.

Table 1 shows the densities of pure heptane at different temperatures. ρ^{Sim} represent values from the GROMACS simulation while ρ^{Asp} represent values from Aspen Plus simulation using the Peng-Robinson method. Thermodynamic values from Aspen plus software have been established to be very close to literature values. The software was adopted to generate experimental values for the densities of the solvent at the selected temperature ranges. Based on the results in Table 1 it was observed that the maximum deviation between the two simulations is 2.32% which was observed at a temperature of 368K and the results also show that as the temperature increases, the deviation also increases. However, since the maximum deviation was just 2.32% within the selected temperature range, it can be concluded that the force field and other parameters selected represent the system well for the simulation to be carried out as a deviation of 2.32% is acceptable. Furthermore, to increase the accuracy of the simulation results, a specific point having the closest density to the experimental value was selected and used within the simulation time frame. The validation of the force field and simulation parameters is continued by determining the diffusion coefficient of the pure solvent (self-diffusion coefficient) within the temperature range selected.

Table 1: Densities of pure heptane at different temperatures from Molecular Dynamics ($\boldsymbol{\rho^{Sim}}$) and Aspen Plus ($\boldsymbol{\rho^{Asp}}$) simulations

T (K)	T^{Sim}/(K)	ρ^{Asp} /(Kgm^{-3})	ρ^{Sim} /(Kgm^{-3})	Error (%)
288	287.817 ± 0.11	690.067	691.947 ± 0.47	0.27
298	297.847 ± 0.15	681.676	682.918 ± 0.76	0.18
303	302.891 ± 0.14	677.427	675.69 ± 0.94	0.26
318	317.882 ± 0.13	664.446	660.113 ± 0.84	0.65
333	332.769 ± 0.15	651.087	645.34 ± 0.74	0.88
343	342.891 ± 0.19	641.949	632.967 ± 1.00	1.40
353	352.818 ± 0.2	632.607	622.221 ± 0.63	1.64
368	367.771 ± 0.18	618.171	603.809 ± 0.8	2.32

Table 2: Diffusion Coefficient of Pure Heptane at Different Temperatures

Temperature K	$D_m^{Sim} \times 10^{-9}$ /(m^{2}s^{-1})	$D_m^{Lit} \times 10^{-9}$ /(m^{2}s^{-1})	Error (%)
288	2.059 ± 0.019		
298	2.036 ± 0.088		
303	2.624 ± 0.052	3.16[a]	16.96
318	3.246 ± 0.164		
333	3.842 ± 0.216	4.01[a]	4.19
343	4.715 ± 0.521		
353	4.727 ± 0.240	5.76[a]	17.83
368	5.926 ± 1.158	6.56[a]	9.66

a: Harris [19]

Table 2 shows the diffusion coefficient value from the simulation (D_m^{Sim}) as well as those from the literature (D_m^{Lit}) specifically from the works of Harris [19]. With respect to the literature values being compared with, the simulation values are observed to be acceptable with the highest error margin being 17.83%. The accuracy of the density and self-diffusion coefficient results from the simulations are considered accurate enough to conclude that the force field selected, and the simulation parameters specified are reliable to proceed with the simulations of the binary systems.

3.2 Binary System

To help validate the results from the simulation, the diffusion of CO_2 in heptane was calculated by three (3) commonly used semi-empirical correlations of Wilke-Chang [20], Hayduk-Laudie [21] and Lusis-Ratcliff [22]. The Wilke-Chang correlation is built upon the readily available properties of dilute solutions. The correlation helps to estimate the diffusion coefficients for engineering purposes. The Wilke-Chang correlation for a solute A in a solution B is given as;

$$D_{AB} = 7.4 \times 10^{-8} \frac{T(\alpha M_B)^{0.5}}{\eta V_A^{0.6}} \tag{7}$$

where D is the diffusion coefficient, T is the temperature, α is the association parameter, M is the molecular weight of the solvent, η is the viscosity of the solvent and V_b is the molar volume of the solute.

Similarly, Lusis and Ratcliff developed a relation for the diffusion coefficient of a binary system as;

$$D_{12} = \frac{8.52\times10^{-15}T}{\eta_2 v_1^{1/3}} \left[1.40 \left(\frac{v_2}{v_1}\right)^{1/3} + \frac{v_2}{v_1}\right] \tag{8}$$

where v_1 and v_2 are the molar volumes of the solute 1 in solvent 2 at their normal boiling points at 1atm. The diffusion coefficient D_{12}, the temperature T and the dynamic viscosity η.

Hayduk and Laudie also presented a relation to predict the diffusivity of solutes in dilute solutions. They developed the correlation using a dilute solution and dissolving 87 different substances, as follows:

$$D_{12} = \frac{13.26(10^{-5})}{\mu_2^{1.4} V_1^{0.589}} \quad (9)$$

where D_{12} is the diffusion coefficient, μ is the viscosity and V is the molar volume, while 1 and 2 signify solute and solvent respectively.

Table 3: Simulated diffusion coefficients of CO_2 in heptane at different temperatures and pressures as well as does from the semi-empirical correlations of Wilke-Chang (*W-C)*, Hayduk-Laudie (*H-L)* and Lusis-Ratcliff *(L-R)*

T(K)	$D_m^{Sim} \times 10^{-9}$ (m^2s^{-1})	$D_m^{W-C} \times 10^{-9}$ (m^2s^{-1})	$D_m^{H-L} \times 10^{-9}$ (m^2s^{-1})	$D_m^{L-R} \times 10^{-9}$ (m^2s^{-1})	W-C Dev. (%)	H-L Dev. (%)	L-R Dev. (%)
			10 bar				
298	7.930±1.17	6.240	5.680	7.336	27.08	39.60	8.10
303	7.009±0.28	6.680	6.105	7.853	4.93	14.80	-10.75
318	9.492±1.16	8.134	7.517	9.563	16.69	26.26	-0.74
333	9.774±0.40	9.829	9.186	1.155	-0.56	6.40	-15.41
343	10.751±0.77	1.112	1.048	1.307	-3.36	2.56	-17.80
353	11.471±0.18	1.258	1.196	1.479	-8.84	-4.12	-22.46
368	14.934±1.00	1.514	1.462	1.780	-1.39	2.09	-16.12
400	19.754±0.91	2.275	2.301	2.674	-13.17	-14.1	-26.14
			20 bar				
298	6.373±0.26	6.251	5.691	7.335	1.94	11.98	-13.12
303	8.629±0.11	6.692	6.116	7.852	28.94	41.08	9.90
318	7.796±0.09	8.149	7.531	9.561	-4.33	3.52	-18.46
333	10.398±0.25	9.847	9.202	1.155	5.60	12.99	-10.00
343	11.497±0.06	1.114	1.050	1.307	3.15	9.48	-12.09
353	14.575±0.02	1.260	1.198	1.479	15.62	21.61	-1.46
368	13.890±0.03	1.517	1.465	1.780	-8.45	-5.22	-21.98
400	19.380±0.03	2.279	2.305	2.674	-14.97	-15.9	-27.53
			80 bar				
298	5.696±0.18	6.288	5.724	7.334	-9.42	-0.49	-22.33
303	6.665±0.19	6.732	6.152	7.852	-0.99	8.34	-15.11
318	7.577±0.32	8.197	7.575	9.561	-7.57	0.03	-20.75
333	8.916±0.83	9.905	9.256	11.552	-9.99	-3.67	-22.82
343	10.597±0.35	11.212	10.562	13.076	-5.48	0.34	-18.95
353	14.056±0.39	12.681	12.055	14.790	10.84	16.60	-4.96
368	14.155±0.21	15.263	14.740	17.800	-7.25	-3.97	-20.48
400	17.300±2.10	22.928	23.187	26.740	-24.55	-25.3	-35.30

Table 3 shows the diffusion coefficients of CO_2 in heptane at different temperatures and pressures. The simulation was repeated three times for each condition with dissimilar initial random seed and the average was taken. The table also shows the diffusion coefficients calculated from the semi-empirical correlations mentioned. Based on the table the diffusion coefficient of the gas in the system increases with an increase in temperature, however the value was observed to be decreasing with pressure increase though not with a large leap. The increase with temperature can be attributed to the fact that, whenever the temperature of a system is increased, the kinetic motion of the particles within the system also increases. With that regard, the gas molecules cover a larger distance at higher temperature in comparison to lower temperature within the same period. This subsequently leads to an increase in the diffusion coefficient. On the other hand, an increase in pressure of a system restricts the movement of the molecules within the system, thus making it harder for the molecules to move and cover a specific distance in comparison to a lower pressure which leads to a reduced diffusion coefficient.

To further visualize the simulation results with those generated from the semi-empirical correlations, a parity plot was made as illustrated in Figures 1, 2 and 3. The parity plot is a scatterplot that effectively compares experimental or simulation data against tabulated data. Data points that fall on the diagonal or close to the diagonal are the most reliable or acceptable in contrast to the experimental or simulation results.

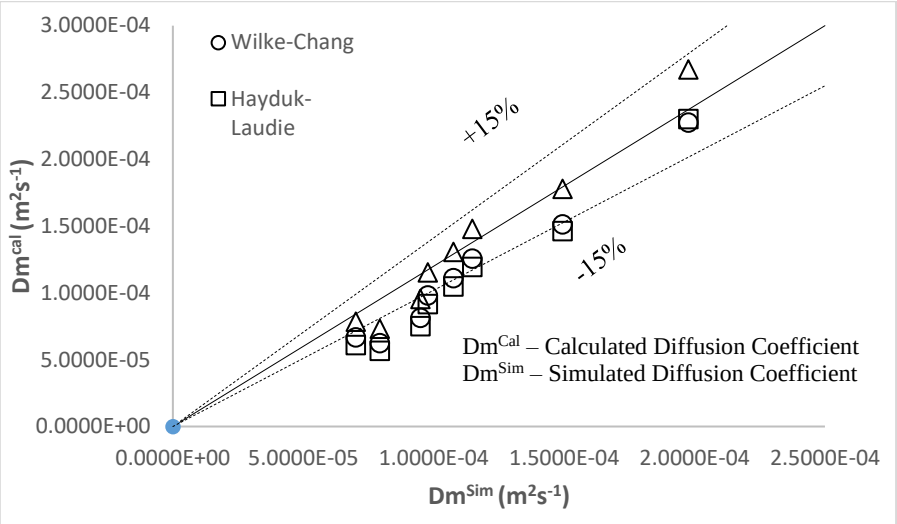

Figure 1: Comparison of simulated and semi-empirically calculated diffusion coefficients of CO_2 in heptane at 10 bar

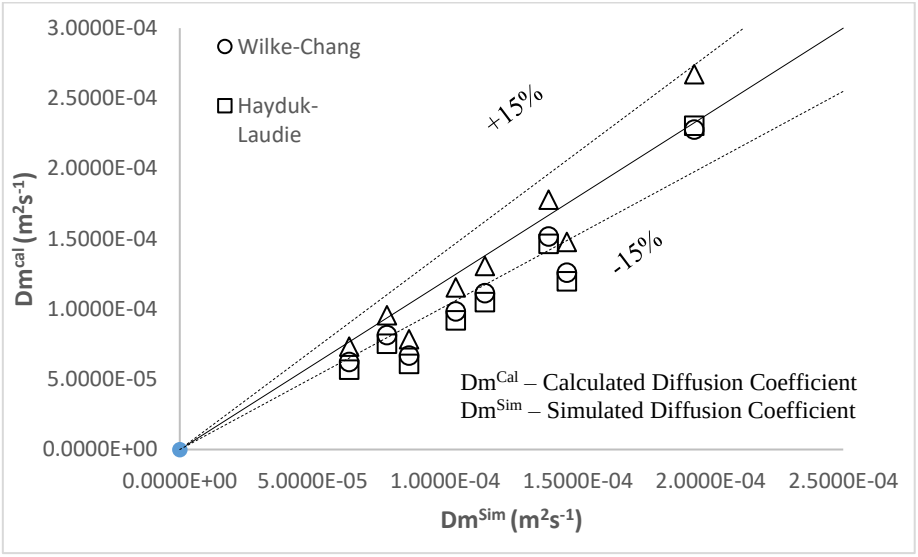

Figure 2: Comparison of simulated and semi-empirically calculated diffusion coefficients of CO_2 in heptane at 20 bar

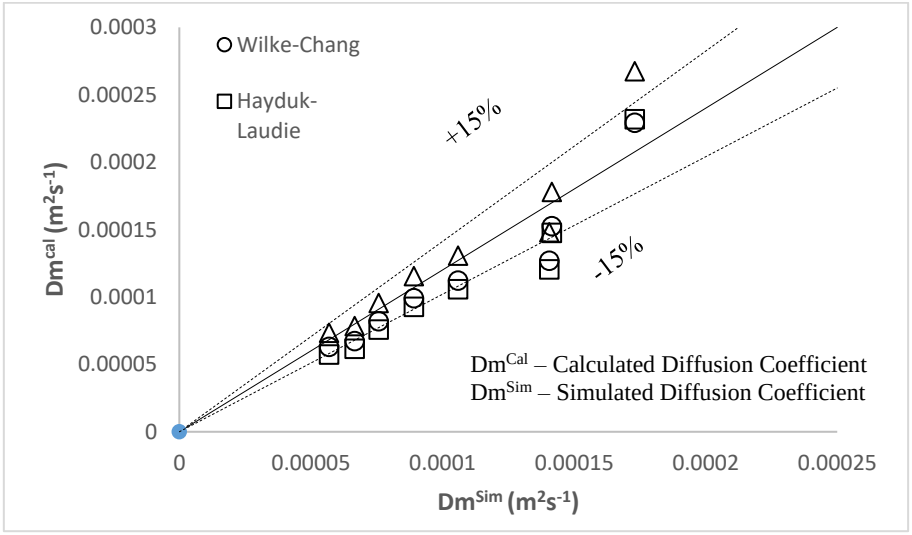

Figure 3: Comparison of simulated and semi-empirically calculated diffusion Coefficients of CO_2 in heptane at 80 bar

Based on the parity plots of the results, it is evident that the Lusis-Ratcliff correlation was more accurate at low temperatures (below 353K) within the pressure range used in this research. But as the temperature increases, the accuracy of the Lusis-Ratcliff's equation begins to drop as the Wilke-Chang's becomes more accurate. Additionally, it was observed that the change in pressure has no significant effect on the performance of the three semi-empirical equations.

This can be ascribed to the fact that, the equations are built on thermodynamic properties such as viscosity, molar volume, temperature, etc. These properties do not have a significant dependency on pressure. And the system investigated is in infinite dilution, i.e the amount of liquid is much higher than the amount of gas, thus the effect of pressure on the whole system was closer to that of the liquid phase only. And it has been established that pressure has very low effect on the thermodynamic properties of a liquid phase [23]. Moreover, the values from the correlation and simulations are in the same magnitude, this is evident that the correlations can be comfortably used at the conditions adopted for the simulation.

3.3 Temperature Dependence

Many researchers have concluded that there is a strong relationship between the diffusion coefficient and temperature [24]. The temperature dependence of the diffusion coefficient has been observed to frequently obey the Arrhenius equation given by Eqn. (10).

$$D = D_0 exp\left(\frac{-E_a}{N_A k_B T}\right) \tag{10}$$

where D is the diffusion coefficient, D_0 is the pre-exponential factor, E_a is the activation energy for diffusion, N_A is the Avogadro's constant, k_B is the Boltzmann constant and T is the temperature. Figures 4, 5 and 6 show the temperature dependence of the diffusion coefficient of CO_2 in heptane at different pressures. All three figures show a good degree of linearity for the temperature dependence of the diffusion coefficient with all having R^2 values of above 0.9.

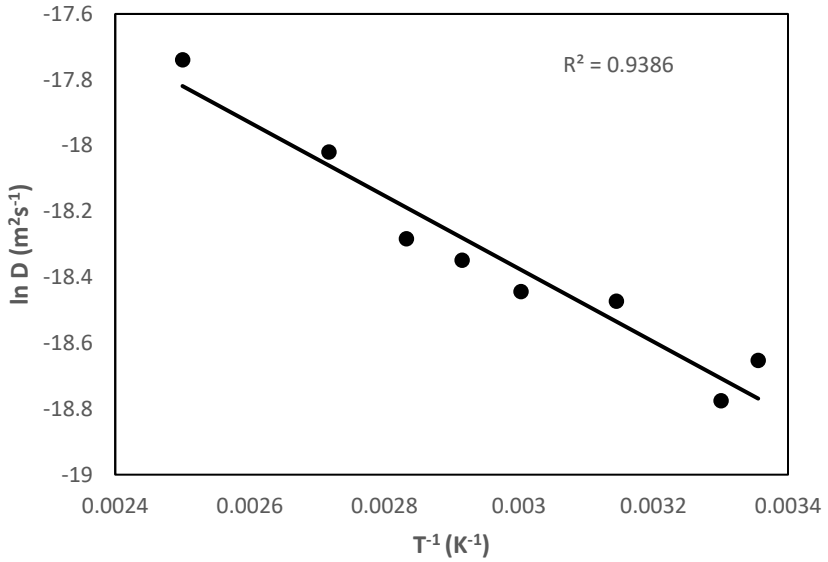

Figure 4: Arrhenius diagram of diffusion coefficients of CO_2 in Heptane at 10 bar

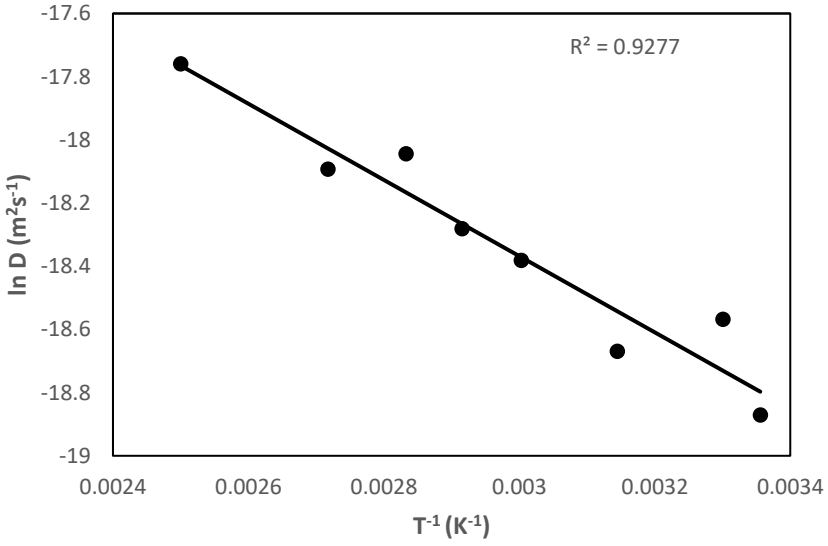

Figure 5: Arrhenius diagram of diffusion coefficients of CO_2 in Heptane at 20 bar

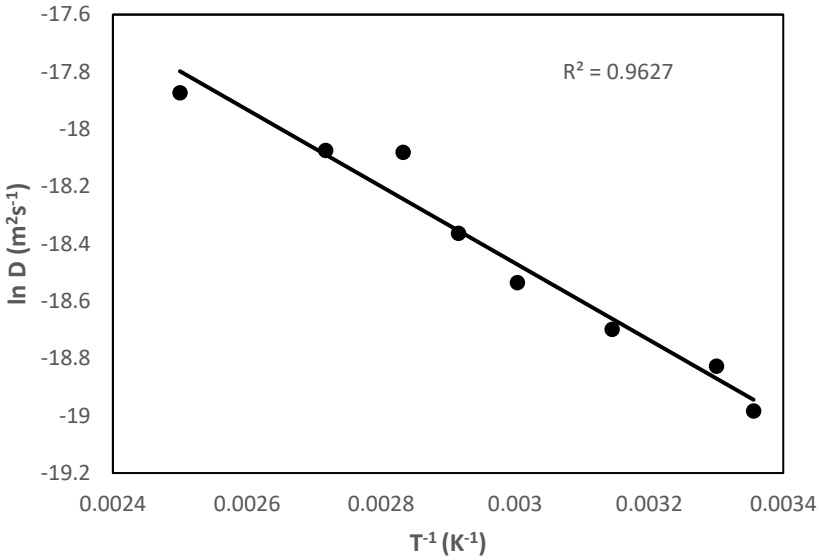

Figure 6: Arrhenius diagram of diffusion coefficients of CO_2 in Heptane at 80 bar

Table 4 shows the activation energies of the system at different pressures. It is evident that the activation energy increases with increase in pressure. This increase with pressure is however expected as the activation energy is the minimum energy required for the gas molecule to initiate the first jump to a new point. An increase in pressure will make the gas molecule require more energy to overcome the pressure barrier to initiate the movement thus leading to an increase in the activation energy.

Table 4: Activation energies of the system at different pressures

Pressure (bar)	**E_a (kJ/mol)**	**R^2**
10	9.228	0.9386
20	10.026	0.9277
80	11.139	0.9627

3.4 Density and Viscosity Dependence

Figure 7 shows the logarithmic relationship between the diffusion coefficients of CO_2 in heptane and the densities between the temperatures of 298K - 400 K and for pressures of 10bar, 20bar and 80bar. The plot shows that the coefficient of diffusion has an exponent relation with the density of the system. As the temperature rises, the density of the heptane decreases and the diffusion coefficient of the CO_2 increases. It has the same trend as the reciprocal of temperature in Figures 4 to 6. this shows that density plays a significant role in determining diffusion coefficients.

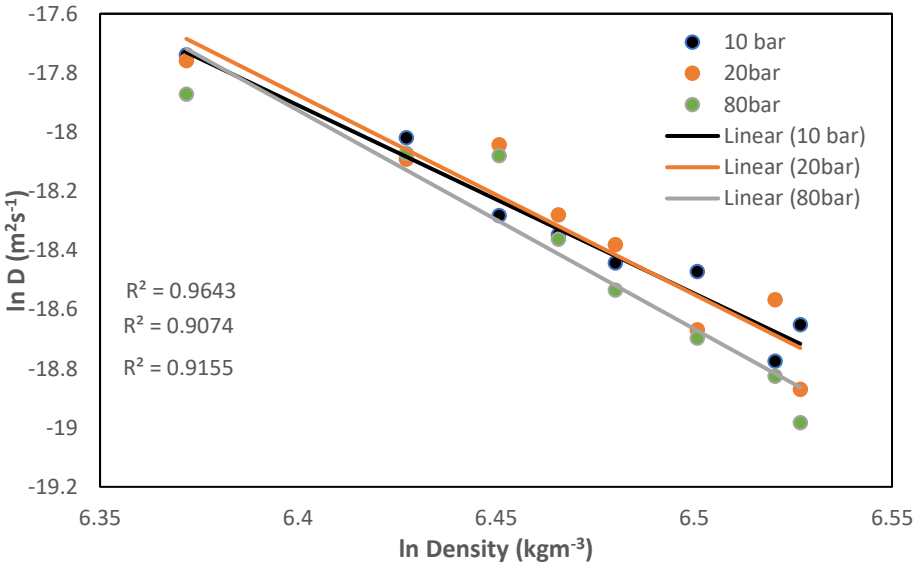

Figure 7: Logarithmic diagram between diffusion coefficients and densities of CO_2 in heptane

Furthermore, from Figure 7 it is also clear that, the effect of pressure in the diffusion coefficient-density relation is less pronounced. As the results at all the three different pressures produce a similar plot with similar slopes.

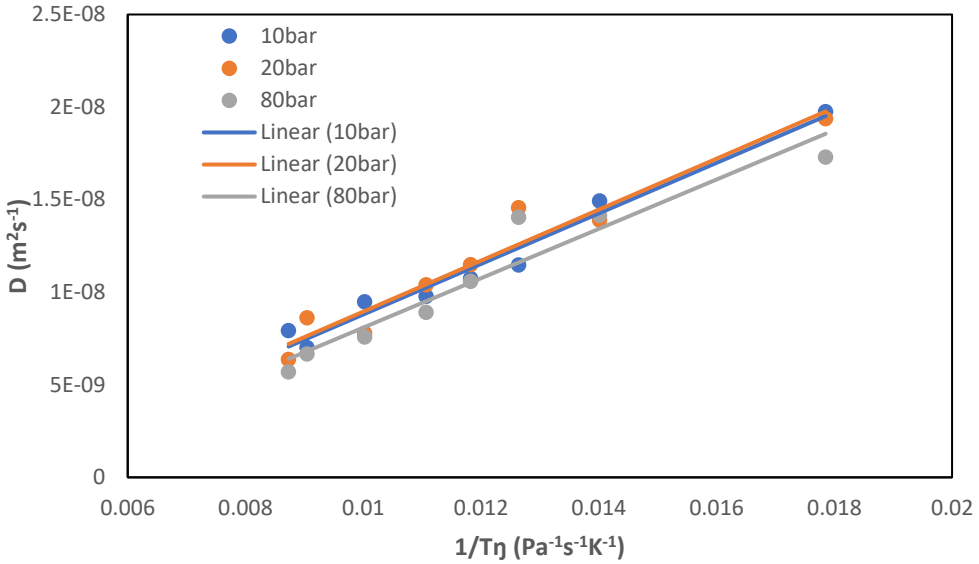

Figure 8: Relationship plot between diffusion coefficient and viscosity of CO_2-Heptane system

As can be seen from Figure 8, diffusion coefficient of CO2 in heptane also have a good linearity with 1/Tη at 298-400K. 1/Tη is a term considering both temperature and viscosity. Viscosity means the friction between the molecules of the fluid. From 298-400K, the temperature increases about 34.23% and the viscosity of the system increases by about 63.18% which all increase the resistance for CO_2 diffusion. While 1/Tη decreases as the temperature increases, the diffusion coefficient of CO_2 still increases. It is possible to conclude that the temperature accelerates the CO_2 diffusion more than the viscosity decelerates it as the temperature surges.

4.0 CONCLUSION

In this work, the diffusion coefficient of CO_2 in heptane has been investigated over the temperature range of 298-400K and at pressures of 10, 20 and 80 bar using molecular dynamics simulation. It was observed that at a pressure of 1 bar and temperature range of 298-400 K, density and diffusion coefficient results from the simulation were consistent with the solute-solvent system. This showed that within the operation condition selected, the force field and simulation parameters selected were sutable for the system. The values of the diffusion coefficients from the simulation were observed to have magnitudes of $10^{-9}m^2s^{-1}$. It was also observed that an increase in temperature increases the kinetic motion of the molecules, which decreases the viscosity of the liquids leading to an increase of the diffusion of CO_2 gas in the solvent from $7.930\times10^{-9}m^2s^{-1}$ to $19.754\times10^{-9}m^2s^{-1}$. An increase in pressure of the system leads to an increase in the restriction of the solute motion within the solvent. Additionally, increase in pressure also increases the density of the solution. These two factors resulted in the decrease in the diffusion coefficient of the carbon dioxide in heptane as a decrease of 28.1% was observed based on a pressure change from 10 – 80 bar.

The semi-empirical correlations of Wilke-Chang, Hayduk-Laudie and Lusis-Ratcliff were used to compare the simulation results of the heptane-carbon dioxide system. The deviation between the simulation results with those from the empirical correlations were observed to be from 1.155 - 27.08% for the Wilke-Chang's, 0.34 – 39.60% for the Hayduk-Laudie's and 1.46 – 27.53% for the Lusis-Ratcliff's which fell within an acceptable error range for the temperature range selected. However, it was observed that, as the temperature of the system was increased, the deviation was also observed to increase. Thus, the semi-empirical correlations can be used satisfactorily for a gas liquid system especially at lower temperatures.

The relationship between the diffusion coefficient and the system temeprature has been observed to obey an Arrhenius type equation with an exponential relationship. The activation energy were recorded to increase with pressure from 9.228 kJ/mol to 11.139 kJ/mol. It was observed that temperature accelerates the carbon dioxide diffusion in heptane while viscosity decelerates it. However, the increase caused by temperature was much greater in comparison to the decrease caused by the viscosity, this led to an overall increase of the diffusion coefficient of the carbondioxide in heptane.

5.0 CONFLICT OF INTEREST

The authors declare no conflicts of interest.

6.0 AUTHORS CONTRIBUTION

A.S Ahmed (Conceptualization; Software; Writing – Original draft; Writing – review & editing)

M.M Ahmed (Supervision, Validation; Data curation)

A.A Bello (Investigation; Resources)

7.0 ACKNOWLEDGEMENTS

This study was not supported by any grants from funding bodies in the public, private, or not-for-profit sectors.

8.0 REFERENCES

[1] O. Massarweh, M. Al-khuzaei, M. Al-Shafi, Y. Bicer, and A. S. Abushaikha, "Blue hydrogen production from natural gas reservoirs: A review of application and feasibility," *Journal of CO2 Utilization*, vol. 70, p. 102438, 2023/04/01/ 2023, doi: https://doi.org/10.1016/j.jcou.2023.102438.

[2] S. Aparicio and M. Atilhan, "Computational Study of Hexamethylguanidinium Lactate Ionic Liquid: A Candidate for Natural Gas Sweetening," *Energy & Fuels*, vol. 24, no. 9, pp. 4989-5001, 2010/09/16 2010, doi: 10.1021/ef1005258.

[3] T. E. Akinola, E. Oko, and M. Wang, "Study of CO2 removal in natural gas process using mixture of ionic liquid and MEA through process simulation," *Fuel*, vol. 236, pp. 135-146, 2019/01/15/ 2019, doi: https://doi.org/10.1016/j.fuel.2018.08.152.

[4] G. E. Halkos and E.-C. Gkampoura, "Reviewing Usage, Potentials, and Limitations of Renewable Energy Sources," *Energies*, vol. 13, no. 11, p. 2906, 2020. [Online]. Available: https://www.mdpi.com/1996-1073/13/11/2906.

[5] P. Balcombe, K. Anderson, J. Speirs, N. Brandon, and A. Hawkes, "The Natural Gas Supply Chain: The Importance of Methane and Carbon Dioxide Emissions," *ACS Sustainable Chemistry & Engineering*, vol. 5, no. 1, pp. 3-20, 2017/01/03 2017, doi: 10.1021/acssuschemeng.6b00144.

[6] S. P. A. Brown, "Natural gas vs. oil in U.S. transportation: Will prices confer an advantage to natural gas?," *Energy Policy*, vol. 110, pp. 210-221, 2017/11/01/ 2017, doi: https://doi.org/10.1016/j.enpol.2017.08.018.

[7] S. Molina, R. Novella, J. Gomez-Soriano, and M. Olcina-Girona, "Study on hydrogen substitution in a compressed natural gas spark-ignition passenger car engine," *Energy Conversion and Management*, vol. 291, p. 117259, 2023/09/01/ 2023, doi: https://doi.org/10.1016/j.enconman.2023.117259.

[8] S. H. A. Rizvi, P. Agrawal, S. Batra, N. Nidhi, and V. Singh, "Assessing urban heat island intensity and emissions with compressed natural gas in non-commercial vehicles," *Urban Climate*, vol. 48, p. 101421, 2023/03/01/ 2023, doi: https://doi.org/10.1016/j.uclim.2023.101421.

[9] A. Demirbas, "The Importance of Natural Gas as a World Fuel," *Energy Sources, Part B: Economics, Planning, and Policy*, vol. 1, no. 4, pp. 413-420, 2006/12/01 2006, doi: 10.1080/15567240500402586.

[10] J. Wang, H. Zhong, C. Liang, X. Chen, and L. Chen, "Molecular dynamics simulation of diffusion and structure of n-alkane/n-alkanol mixtures at infinite dilution," *Journal of Molecular Liquids*, vol. 223, pp. 489-496, 2016/11/01/ 2016, doi: https://doi.org/10.1016/j.molliq.2016.08.091.

[11] H. K. Chilukoti, G. Kikugawa, and T. Ohara, "Self-diffusion Coefficient and Structure of Binary n-Alkane Mixtures at the Liquid–Vapor Interfaces," *The Journal of Physical Chemistry B*, vol. 119, no. 41, pp. 13177-13184, 2015/10/15 2015, doi: 10.1021/acs.jpcb.5b07189.

[12] Z. A. Makrodimitri, D. J. M. Unruh, and I. G. Economou, "Molecular Simulation of Diffusion of Hydrogen, Carbon Monoxide, and Water in Heavy n-Alkanes," *The Journal of Physical Chemistry B*, vol. 115, no. 6, pp. 1429-1439, 2011/02/17 2011, doi: 10.1021/jp1063269.

[13] G. Kamath, N. Lubna, and J. J. Potoff, "Effect of partial charge parametrization on the fluid phase behavior of hydrogen sulfide," *The Journal of Chemical Physics*, vol. 123, no. 12, p. 124505, 2005, doi: 10.1063/1.2049278.

[14] X. Zhao and H. Jin, "Investigation of hydrogen diffusion in supercritical water: A molecular dynamics simulation study," *International Journal of Heat and Mass Transfer*, vol. 133, pp. 718-728, 2019/04/01/ 2019, doi: https://doi.org/10.1016/j.ijheatmasstransfer.2018.12.164.

[15] M. Seyyedattar, S. Zendehboudi, and S. Butt, "Invited review - Molecular dynamics simulations in reservoir analysis of offshore petroleum reserves: A systematic review of theory and applications," *Earth-Science Reviews*, vol. 192, pp. 194-213, 2019/05/01/ 2019, doi: https://doi.org/10.1016/j.earscirev.2019.02.019.

[16] M. P. Allen, "Introduction to molecular dynamics simulation," *Computational Soft Matter: From Synthetic Polymers to Proteins*, vol. 23, pp. 1-28, 2004.

[17] O. A. Moultos, I. N. Tsimpanogiannis, A. Z. Panagiotopoulos, J. P. M. Trusler, and I. G. Economou, "Atomistic Molecular Dynamics Simulations of Carbon Dioxide Diffusivity in n-Hexane, n-Decane, n-Hexadecane, Cyclohexane, and Squalane," *The Journal of Physical Chemistry B*, vol. 120, no. 50, pp. 12890-12900, 2016/12/22 2016, doi: 10.1021/acs.jpcb.6b04651.

[18] "Groningen Machine for Chemical Simulation." https://www.gromacs.org/ (accessed 2021).

[19] K. R. Harris, "Temperature and density dependence of the self-diffusion coefficient of n-hexane from 223 to 333 K and up to 400 MPa," *Journal of the Chemical Society, Faraday Transactions 1: Physical Chemistry in Condensed Phases*, 10.1039/F19827802265 vol. 78, no. 7, pp. 2265-2274, 1982, doi: 10.1039/F19827802265.

[20] C. R. Wilke and P. Chang, "Correlation of diffusion coefficients in dilute solutions," *AIChE Journal*, vol. 1, no. 2, pp. 264-270, 1955, doi: 10.1002/aic.690010222.

[21] W. Hayduk and B. S. Minhas, "Correlations for prediction of molecular diffusivities in liquids," *The Canadian Journal of Chemical Engineering*, vol. 60, no. 2, pp. 295-299, 1982, doi: 10.1002/cjce.5450600213.

[22] J. G. Liu, G. S. Luo, S. Pan, and J. D. Wang, "Diffusion coefficients of carboxylic acids in mixed solvents of water and 1-butanol," *Chemical Engineering and Processing: Process Intensification*, vol. 43, no. 1, pp. 43-47, 2004/01/01/ 2004, doi: https://doi.org/10.1016/S0255-2701(02)00182-4.

[23] C. Giraudet, T. Klein, G. Zhao, M. H. Rausch, T. M. Koller, and A. P. Fröba, "Thermal, Mutual, and Self-Diffusivities of Binary Liquid Mixtures Consisting of Gases Dissolved in n-Alkanes at Infinite Dilution," *The Journal of Physical Chemistry B*, vol. 122, no. 12, pp. 3163-3175, 2018/03/29 2018, doi: 10.1021/acs.jpcb.8b00733.

[24] Y. Zhao, Y. Feng, and X. Zhang, "Molecular simulation of CO2/CH4 self- and transport diffusion coefficients in coal," *Fuel*, vol. 165, pp. 19-27, 2016/02/01/ 2016, doi: https://doi.org/10.1016/j.fuel.2015.10.035.